

## Plastic Deformation of Alkali Halide Crystals at High Pressure: Work-Hardening Effects\*

L. A. DAVIS† AND R. B. GORDON

Department of Geology and Geophysics, Yale University, New Haven, Connecticut 06520

(Received 15 May 1969)

The influence of hydrostatic pressure on the plastic deformation of alkali halide single crystals at large strain has been observed. The rates of work hardening in stages I and II are approximately independent of pressure in LiF, NaCl, and KCl, but both are doubled at 4.3 kbar in KI. In stage II the fractional increase of plastic flow stress at high pressure in an interrupted compression test,  $\delta\sigma/\sigma$ , is accounted for by the pressure-induced increase in elastic constants in all the alkali halides examined. Evidently, the strength in stage II is controlled by elastic interactions. The stress at the onset of stage III,  $\sigma_{III}$ , in the deformation of NaCl at 4.3 kbar is about half that at 1 atm; it is reduced slightly in KCl and is unchanged in KI. Deformation proceeds at lower stresses in stage III in NaCl and KCl under 4.3 kbar, and if compression at 1 atm in this stage is interrupted and reinitiated at 4.3 kbar, pronounced work softening is observed. The dependence of flow stress on pressure in stage III at constant structure,  $(\delta\sigma/\sigma)_s$ , is small and less than that expected from the pressure-induced change of elastic constants. The negative pressure dependence of  $\sigma_{III}$  and the small  $(\delta\sigma/\sigma)_s$  in stage III may be explained in terms of thermally activated cross slip of screw dislocations when stacking faults on the primary slip plane cause a strong local dilation of the lattice.

### INTRODUCTION

Alkali halide single crystals with the NaCl structure exhibit the three-stage stress-strain ( $\sigma$ - $\epsilon$ ) curve shown schematically in Fig. 1. Stages I and II are approximately linear, with the rate of work hardening,  $d\sigma/d\epsilon$ , as much as ten times greater in stage II. Stage III exhibits a rate of work hardening which is smaller than in stage II and which decreases slowly with continuing strain. The onset of stage II is taken as the intersection of the linear extrapolations of stages I and II; stage III begins, by definition, when the  $\sigma$ - $\epsilon$  curve deviates by 1% strain from the linear extrapolation of stage II. We examine here the influence of hydrostatic pressure on the plastic deformation of several of the alkali halides in an attempt to identify the strength controlling mechanisms. Two types of experiments are conducted: (1) continuous  $\sigma$ - $\epsilon$  curves are recorded at 1 atm and 4.3 kbar, and (2) interrupted tests are performed in which the deformation of a crystal at pressure  $P_1$  is halted, the pressure changed to  $P_2$ , and the deformation then continued at  $P_2$ , perhaps with a change of flow stress or rate of work hardening. Intercomparison of these two types of experiments enables one to determine the separate dependence of flow stress and dislocation structure on pressure after the method used by Cottrell and Stokes<sup>1</sup> in their experiments with temperature changes. The authors have previously reported results for the fractional change of flow stress with pressure in interrupted tests in stage I for annealed and radiation-hardened alkali halides<sup>2</sup>; interrupted tests here will be limited to stages II and III.

\* Research supported by the U.S. Army Research Office (Durham).

† Present address: Materials Research Center, Allied Chemical Corporation, Morristown, N.J. 07960.

<sup>1</sup> A. H. Cottrell and R. J. Stokes, Proc. Roy. Soc. (London) **A233**, 17 (1955).

<sup>2</sup> L. A. Davis and R. B. Gordon, J. Appl. Phys. **39**, 3885 (1968).

### EXPERIMENTAL PROCEDURE

Plastic deformation of alkali halide single crystals at 4.3 kbar is achieved in the *minilester*, previously described,<sup>2,3</sup> which permits uniaxial stress-strain compression testing of samples held under hydrostatic pressure. The uniaxial force is measured by a strain-gauge-type load cell. In the present work both a previously used load cell (L.C. #4)<sup>4</sup> and a second load cell having similar properties (L.C. #6; 1 atm calibration =  $1.8 \times 10^{-6}/N$ ) are used. The materials tested are LiF, NaCl, KCl, and KI. Compression samples are cleaved from large blocks themselves cleaved from annealed crystals by the Harshaw Chemical Company. Sample dimensions are usually about  $1.3 \times 0.5 \times 0.4$  cm, which is approximately half the size of those previously used; for the compression rate used (0.009 cm/min), the compressive strain rate is  $\sim 1 \times 10^{-4}/\text{sec}$ . The ends of the samples are lubricated with 0.05-mm-thick sheets of Teflon to minimize the formation of cleavage cracks parallel to the compression direction. Except at very large strains, where they become catastrophic, these cracks have no effect on the  $\sigma$ - $\epsilon$  curve. After heavy deformation ( $\sim 2$  mm in a 12.7-mm-long sample) the sample ends remain parallel to within about 0.08 mm. Stress birefringence observations of lightly deformed samples indicate that slip occurs on both possible slip planes of one orthogonal  $\{110\}$   $\langle 1\bar{1}0 \rangle$  set; the two oblique systems may operate simultaneously at low deformations in LiF. After heavy deformation, the specimens assume a shape characteristic of a predominance of slip on a single

<sup>3</sup> R. B. Gordon and L. F. Mike, Rev. Sci. Instrum. **38**, 541 (1967).

<sup>4</sup> An error in the 1 atm calibration of L.C. #4 has been detected. The load calibration of L.C. #4 noted in Ref. 2 is low by a factor of 1.4, i.e., it is  $1.89 \times 10^{-6}/N$  rather than  $1.35 \times 10^{-6}/N$ . Consequently, the stresses calculated in Ref. 2 are too high by a factor of 1.4. However, the absolute value of the stress is not important in Ref. 2.



TABLE I. Work-hardening parameters (1 atm).

	$\sigma_0$ (bars)	$N_{\theta I}^a$	$\theta_I$ bars/u.s.s. <sup>b</sup>	$\frac{\epsilon_{II}}{\%}$ (shear)	$N_{\theta II}^a$	$\theta_{II}$ bars/u.s.s.	$\sigma_{III}$ bars	$\frac{\epsilon_{III}-\epsilon_{II}}{\%}$ (shear)	$K_s$ Mbar	$\theta_{II}/K_s$ $\times 10^3$	$\theta_I/K_s$ $\times 10^3$
LiF	7 $\pm$ 1	10	120 $\pm$ 10 <sup>a</sup>	10 $\pm$ 3	1	1000 (4.3 kbar)	...	...	0.46	2.2	0.3
NaCl	3 $\pm$ 1	12	170 $\pm$ 50	5 $\pm$ 2	4	550 $\pm$ 30	90 $\pm$ 10	15 $\pm$ 5	0.15	3.7	1.1
KCl	4 $\pm$ 1	5	280 $\pm$ 40	3 $\pm$ 2	6	340 $\pm$ 40	45 $\pm$ 8	11 $\pm$ 3	0.10	3.4	2.8
KI	5 $\pm$ 1	11	180 $\pm$ 40	4 $\pm$ 2	6	270 $\pm$ 25	25 $\pm$ 5	6 $\pm$ 3	0.065	4.2	2.8

<sup>a</sup>  $N$  = number of measurements averaged in computing slopes;  $N_{\theta I}$  includes some samples studied previously (Ref. 2).

<sup>b</sup> Bars/unit shear strain.

<sup>a</sup> Limits are average deviation for  $\theta_I$  and  $\theta_{II}$  and maximum deviation for other parameters.

slip system, in agreement with the observations of Davidge and Pratt<sup>5</sup> and Hesse<sup>6</sup> on NaCl. To remove effects due to varying specimen geometry, the lengths of crystals whose  $\sigma$ - $\epsilon$  curves at 1 atm and 4.3 kbar are to be compared are carefully matched to within  $\pm 0.02$  mm and their areas, to within  $\pm 4\%$ .

### RESULTS

Typical 1 atm, room-temperature  $\sigma$ - $\epsilon$  curves observed for LiF, NaCl, KCl, and KI are given in Fig. 2. The stress and strain are calculated as  $\sigma_s = \sigma_c/2$  and  $\epsilon_s = 2\epsilon_c = 2\Delta l/l_0$ , where subscript  $s$  and  $c$  refer to shear and compression respectively. Work-hardening parameters are listed in Table I. A systematic decrease in  $\theta_{II}$ , the slope of stage II, ( $\epsilon_{III} - \epsilon_{II}$ ), the range of stage II, and  $\sigma_{III}$  is observed in the order of decreasing  $K_s$ , where  $K_s = \{\frac{1}{2}(c_{11} - c_{12})/c_{44}\}^{1/2}$  is the stress-field elastic constant for a screw dislocation in the NaCl structure.<sup>7</sup> The critical resolved shear stress,  $\sigma_0$ , and  $\epsilon_{II}$ , the range of stage I, are greatest in LiF while  $\theta_I$ , the slope of stage I,

is smallest, but variation of these parameters in the other alkali halides does not appear systematic. The value of  $\theta_{II}$  listed for LiF is obtained from one experiment at 4.3 kbar as, due to the intervention of cracking, stage II does not fully develop at 1 atm. It is probable that  $\theta_{II}$  is comparable at 1 atm and 4.3 kbar in LiF. To account for differences in elastic properties,  $\theta_I$  and  $\theta_{II}$  may be divided by  $K_s$ . The ratio  $\theta_{II}/K_s$  is roughly constant at  $(3 \pm 1) \times 10^{-3}$ ;  $\theta_I/K_s$  varies by a factor of 10.

The effect of 4.3-kbar pressure on the  $\sigma$ - $\epsilon$  curves for LiF, NaCl, KCl, and KI is shown in Figs. 3-6. The typical reproducibility of the deformation curves is indicated in Fig. 4 for NaCl. Figure 5 for KCl represents data for six specimens, with three each run at 1 atm and 4.3 kbar. In Fig. 6, for KI, the curves are averages for four crystals at each pressure. In each case, the error bars represent the maximum spread of the data.

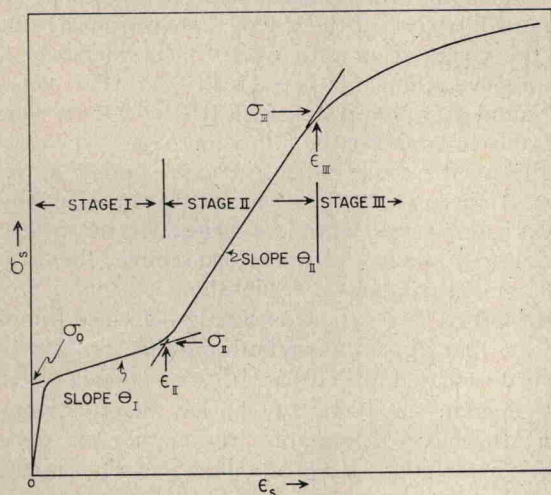


FIG. 1. A schematic, single-crystal stress-strain curve showing three stages of work hardening.

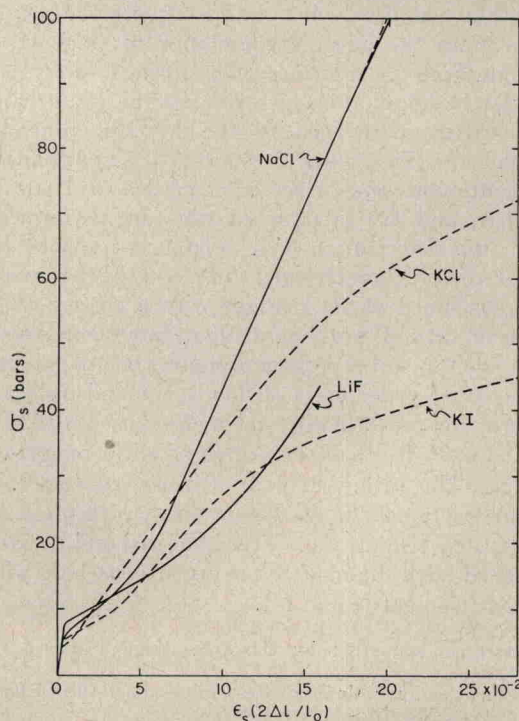


FIG. 2. Typical compression stress-strain curves at 1 atm and room temperature for NaCl, KCl, LiF, and KI. Dashed line for NaCl is extrapolation of stage II.

<sup>5</sup> R. W. Davidge and P. L. Pratt, Phys. Status Solidi 6, 759 (1964).

<sup>6</sup> J. Hesse, Phys. Status Solidi 9, 209 (1965).

<sup>7</sup> A. J. E. Foreman, Acta Met. 3, 322 (1955).